molecular pharmaceutics

ARTICLE

pubs.acs.org/molecularpharmaceutics

A Novel Peptide Probe for Imaging and Targeted Delivery of Liposomal Doxorubicin to Lung Tumor

Xiaofeng He,[‡,†] Moon-Hee Na,[‡,†] Jin-Sook Kim,[†] Ga-Young Lee,[†] Jae Yong Park,[†,§] Allan S. Hoffman,[∥,⊥] Ju-Ock Nam,[#] Su-Eun Han,[▽] Ga Yong Sim,[▽] Yu-Kyoung Oh,[○] In-San Kim,[†] and Byung-Heon Lee*[,†]

[†]Department of Biochemistry and Cell Biology and Cell & Matrix Research Institute, [§]Department of Internal Medicine, and [∥]WCU Program, School of Medicine, Kyungpook National University, Daegu 700-421, Korea

[⊥]Department of Bioengineering, University of Washington, Seattle, Washington 98195-5061, United States

[#]Department of Ecological Environment Conservation, Kyungpook National University, Sangju-Si, Gyeongsangbuk-Do 742-711, Korea

[▽]School of Life Sciences and Biotechnology, Korea University, Seoul 136-701, Korea

[○]College of Pharmacy, Seoul National University, Seoul 151-742, Korea

ABSTRACT: Targeted delivery of imaging agents and therapeutics to tumors would provide early detection and increased therapeutic efficacy against cancer. Here we have screened a phage-displayed peptide library to identify peptides that selectively bind to lung tumor cells. Evaluation of individual phage clones after screening revealed that a phage clone displaying the CSNIDARAC peptide bound to H460 lung tumor cells at higher extent than other phage clones. The synthetic CSNIDARAC peptide strongly bound to H460 cells and was efficiently internalized into the cells, while little binding of a control peptide was seen. It also preferentially bound to other lung tumor cell lines as compared to cells of different tumor types. *In vivo* imaging of lung tumor was achieved by homing of fluorescence dye-labeled CSNIDARAC peptide to the tumor after intravenous injection into mice. *Ex vivo* imaging and microscopic analysis of isolated organs further demonstrated the targeting of CSNIDARAC peptide to tumor. The CSNIDARAC peptide-targeted and doxorubicin-loaded liposomes inhibited the tumor growth more efficiently than untargeted liposomes or free doxorubicin. *In vivo* imaging of fluorescence dye-labeled liposomes demonstrated selective homing of the CSNIDARAC-liposomes to tumor. In the same context, higher levels of doxorubicin and apoptosis in tumor tissue were observed when treated with the targeted liposomes than untargeted liposomes or free doxorubicin. These results suggest that the CSNIDARAC peptide is a promising targeting probe that is able to direct imaging agents and therapeutics to lung tumor.

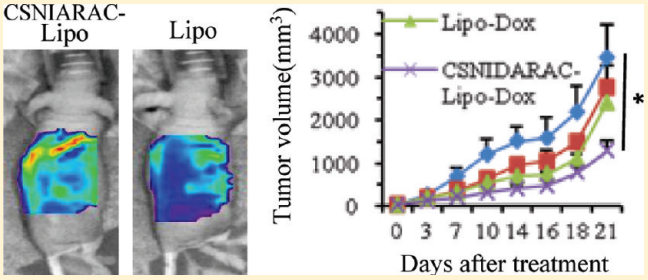

KEYWORDS: drug delivery, imaging, liposomal doxorubicin, lung tumor, peptide probe, phage display

INTRODUCTION

Lung cancer is the leading cause of cancer deaths in the United States and worldwide for both men and women.[1] The high mortality may be caused by late detection of lung cancer due to the lack of adequate diagnostic biomarkers and by unsatisfactory treatment efficiency of conventional chemotherapeutic agents due to their high degree of cytotoxicity. One promising approach to improve treatment efficiency is the targeted therapy using anticancer drugs that act on tumor-specific targets. For example, a small molecule inhibitor of epidermal growth factor (EGF) receptor, such as Gefitinib, has shown promising therapeutic effects in patients with lung cancer.[2] However, Gefitinib is effective only in patients with mutant EGF receptor, and the population of such patients accounts for only a small portion of the whole population of patients with lung cancer,[3] limiting the popular use of the drug.

In this regard, the targeted delivery of therapeutic agents to lung tumors would be another promising approach. This may be achieved by coupling therapeutic agents with targeting probes such as antibodies, RNA aptamers, and peptides, which direct the drugs to tumor tissue and thus enhance the therapeutic efficacy. Both conventional chemotherapeutic agents and novel targeted therapeutic agents would be available for this purpose. For example, transferrin or an antibody to transferrin receptor that is known to be overexpressed in many types of cancer has been widely used for drug delivery.[4,5] An RNA aptamer against prostate-specific membrane antigen has been used for directing nanoparticles to prostate cancer.[6] A typical example of a peptide

[‡] These authors contributed equally.

Received: August 12, 2010
Accepted: January 11, 2011
Revised: November 19, 2010
Published: January 11, 2011

probe for drug delivery to tumors is the RGD peptide that binds to $\alpha v\beta 3$ integrin of tumor endothelial cells.[7] Octreotide, an octapeptide analogue of somatostatin,[8] has also been used for diagnosis, radionuclide therapy, and drug delivery to neuroendocrine tumors.[9−11] When compared to antibodies, peptides appear to have advantages as a targeting probe for both imaging and drug delivery. They have smaller sizes and better tissue penetration than antibodies, and coupling therapeutics or imaging agents with peptides is easier than that with antibodies.[12]

Currently, ^{18}F-labeled fluorodeoxyglucose (FDG)-positron emission tomography (PET) imaging is used for the detection of cancer, which is based on the increased glucose utilization of cancer cells. FDG-PET imaging is very sensitive at cancer detection. However, FDG uptake is relatively nonspecific, since it is also increased in inflammatory lesions. To overcome this limitation, imaging probes that are specific to target cells or molecules in tumor microenvironment are required. In this regard, peptide probes that can selectively bind to targets in tumor tissue would be useful tools for molecular imaging and early detection of cancer. Monomeric or multimeric RGD peptide, for example, has been labeled with ^{18}F and employed for the imaging of tumor angiogenesis.[13,14]

Phage display has successfully selected peptides that are specific for molecular signatures or biomarkers at tumor tissue and tumor vasculature. *In vivo* screening that involves intravenous administration of phage libraries has identified peptides that home to diverse pathologic tissues such as cancer,[15] tumor blood vessels,[7] and ischemic cerebral cortex.[16] *Ex vivo* screening that involves the binding of phages to primary tissues has identified peptides that specifically bind to the target tissue, such as dysplastic colon mucosa.[17] Moreover, *in vitro* screening that involves the binding of phages to cultured cells has identified peptides that are specific to tumor cells, such as bladder tumor cells,[18] lung tumor cell,[19,20] and glioma cells.[21]

In this study, we describe the identification of a lung tumor cell-binding peptide using *in vitro* screening of phage-displayed peptide library and its application to both *in vivo* imaging and targeted drug delivery to lung tumor.

MATERIALS AND METHODS

Cell Lines and Cell Cultures. H460 cells, A549 cells, H226 cells, and SNU484 cells were grown in RPMI-1640 medium containing 10% fetal bovine serum (FBS). MBA-MD231and HT29 were grown in Dulbecco's modified Eagle's medium (DMEM) containing 10% FBS. BEAS-2B cells were grown in DMEM/F12 containing 10% FBS.

Biopanning of a Phage-Displayed Peptide Library. A T7 phage library displaying CX_7C (C, cysteine; X, any amino acid) random peptides (Novagen, Madison, WI, USA) was used for biopanning. H460 cells (1×10^6 cells) were seeded onto a well/6-well plate and allowed to grow overnight. Cells were blocked at 37 °C for 30 min with RPMI-1640 medium containing 1% bovine serum albumin (BSA). The phage library at 1×10^9 plaque forming units (pfu) was incubated with cells at 4 °C for 1 h. After removing unbound phages with phosphate-buffered saline (PBS) containing 1% BSA, cell-bound phages were eluted by 1% NP-40 lysis solution and BL21 bacteria culture. Eluted phages were amplified and subjected to consecutive rounds of biopanning. After four rounds, forty-seven phage clones from the third and fourth rounds were randomly picked. Their peptide-coding DNA inserts were amplified by PCR and sequenced. Fluorescein isothiocyanate (FITC)-conjugated peptides were synthesized using a standard Fmoc method (Peptron Inc., Daegeon, Korea)

Phage Cell-Binding Enzyme-Linked Immunosorbent Assay (ELISA). Cells (1×10^4 cells) were seeded in a well/96-well plate and allowed to grow overnight. Cells were blocked with a medium containing 1% BSA at 4 °C for 30 min. Individual phage clones (1×10^9 pfu) were added and incubated at 4 °C for 1 h. The cells were washed with PBS and incubated with anti-T7-horse radish peroxidase antibody (Novagen) at room temperature for 1 h. The cells were washed with PBS and incubated with the Turbo-TMB (Pierce, Rockford, IL, USA) enzyme substrate at room temperature for 15 min. Reaction was terminated by adding 2 M H_2SO_4 and measured with a microplate reader at 450 nm wavelength.

Immunofluorescence Assays of Peptide Binding and Internalization. Cells were plated at 1×10^4 cells onto a well/8-well chamber slide. After overnight culture, cells were blocked with a culture medium containing 1% BSA at 37 °C for 30 min and then incubated with a FITC-conjugated peptide in serum-free culture medium at 37 °C for 1 h. After washing, cells were fixed with 4% paraformaldehyde and incubated with 4′,6′-diamidino-2- phenylindole (DAPI, Sigma-Aldrich, St. Louis, MO, USA) for nuclear staining. The chamber slides were mounted with Antifade reagent (Invitrogene, Carlsbad, CA, USA) and visualized under a fluorescent microscope (Zeiss, Oberkochen, Germany).

Flow Cytometry Analysis of Peptide Binding. Cells were grown to 70% to 80% confluence, harvested, and suspended in culture medium. Cells were incubated with culture medium containing 1% BSA at 37 °C for 30 min for blocking and then with a FITC-conjugated peptide in serum-free medium at 37 °C for 1 h. After washing with PBS, cells were subjected to flow cytometry (BD Bioscience, San Jose, CA, USA).

***In Vivo* and *ex Vivo* Fluorescence Imaging of Peptide Homing and Immunohistochemistry.** All animal experiments were approved by Kyungpook National University Animal Experiment Ethics Committee. H460 tumor cells (5×10^6 cells) were subcutaneously injected into the right flank of 5 week-old BALB/c *nu/nu* female mice. Tumor-bearing mice were injected via tail vein with 200 nanomoles of peptide in PBS. *In vivo* fluorescence images were taken using Optix imaging system (ART Inc., Montreal, Canada). After 2 h of incubation, tumor and organs were isolated, and *ex vivo* fluorescence images were taken using Optix. After taking imaging, tumor and organs were fixed with 4% paraformaldehyde for 2 h and frozen for cryosection. Tissue slides were incubated with a mounting medium containing DAPI for nuclear staining and observed under a fluorescence microscope.

Preparation of Peptide-Labeled Liposomal Doxorubicin. Egg L-α-phosphatidylcholine (PC), egg L-α-phosphatidyl-DL-glycerol (PG), 1,2-diacyl-*sn*-glycero-3-phosphoethanolamine-*N*-[methoxy(polyethylene glycol)-2000] ($mPEG_{2000}$-DSPE), 1,2-distearoyl-*sn*-glycero-3-phosphoethanolamine-*N*-[maleimide-(polyethylene glycol)2000] (maleimide-PEG_{2000}-DSPE) and 1,2-dioleoyl-*sn*-glycero-3-phosphoethanolamine (DOPE) were purchased from Avanti Polar Lipids (Alabaster, AL, USA). Fifteen micromoles of peptide was dissolved in water at room temperature. Dithiothreitol (DTT) was added into the peptide solution at a concentration of 1 mM and stirred for 1 h. Maleimide-PEG_{2000}-DSPE was dissolved in dimethyl sulfoxide, added into the reaction mixture and then stirred at 4 °C for 16 h in the presence of DTT. The reaction mixture was placed in a rotary evaporator to remove the solvent, and then ethyl acetate was added. The residue was purified by dialysis against water. The

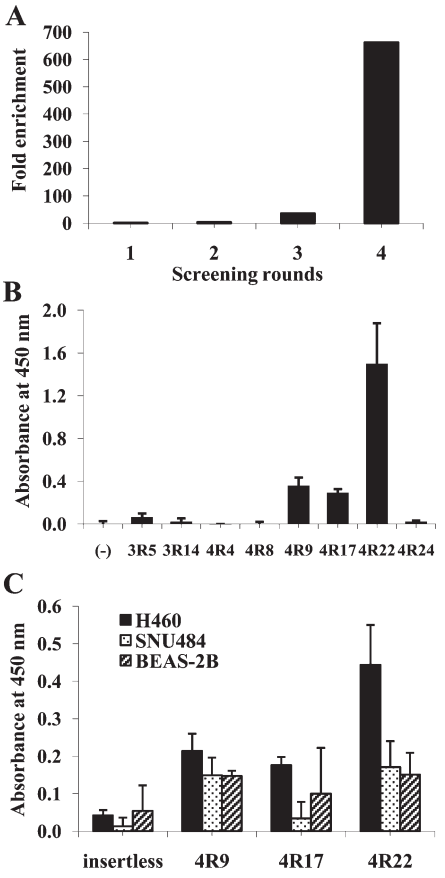

Figure 1. Screening of a phage library for peptides that bind to H460 lung tumor cells. (A) A T7 phage-displayed peptide library was incubated with H460 cells. Cell-bound phages were recovered, amplified, and used for the next round of selection. Bars represent the fold enrichment of phage titer at each round relatively over the titer at the first round. (B) Phage cell-binding ELISA. Individual phage clones were incubated with H460 cells. Cell-bound phages were detected with peroxidase-conjugated antiphage antibody. Bars represent the absorbance at 450 nm of each phage clone as mean ± SD of data obtained from two separate experiments performed in triplicate. (C) Three phage clones (4R9, 4R17, and 4R22) were incubated with the indicated cells. Binding of each phage clone was measured by the phage cell-binding ELISA. Bars represent the absorbance at 450 nm of each phage clone as mean ± SD of data obtained from two separate experiments performed in triplicate.

purification resulted in the formation of peptide-PEG_{2000}-DSPE as a colorless viscous oil.

For the preparation of Cy7.5 near-infrared fluorescence dye-labeled liposomes, 15 μmol of Cy7.5 hydroxysuccinimide was dissolved in water and added into dimethylformamide dissolving DOPE at room temperature. The mixture was stirred for 16 h, and the solvent was completely removed by evaporation. Ethyl acetate was added to the mixture for washing. The crude residue was purified by column chromatography. The purification resulted in the formation of Cy7.5-DOPE as a green viscous oil.

Liposomes were prepared by a multilamella vesicle method with a slight modification. For the preparation of liposome solution, PC, PG, cholesterol, DOPE and peptide-PEG_{2000}-DSPE were dissolved at a molar ratio of 5:5:5:0.1:0.2 in chloroform. PG was used for negative surface charge of liposomes. The lipid mixtures were placed in a rotary evaporator under reduced pressure to remove the chloroform, which resulted in the formation of thin lipid films. The films were hydrated with 20 mM 4-(2-hydroxyethyl)-1-piperazineethanesuffonic acid (HEPES) buffer, pH 7.4, by vortexing. The resulting multilamellar vesicles were sized by repeated extrusion through polycarbonate membrane filters with the pore size of 200 nm. To load doxorubicin into the negatively charged liposomes, 500 μg of doxorubicin was mixed with 1 mL of the liposome solutions (PC:PG:cholesterol:DOPE:peptide-PEG-DSPE = 5:5:5:0.1:0.2 μmol/mL). Doxorubicin, which has a positive charge at pH 7.4 due to its primary amine group, was complexed onto the surface of negatively charged liposomes by electrostatic interaction. Excess amount of doxorubicin was removed by gel filtration through a Sephadex G-25 M column (GE Healthcare, Piscataway, NJ, USA).

Table 1. Phage-Displayed Peptide Sequences Selected for Binding to H460 Lung Tumor Cells

phage clone	peptide sequence
3R5	CDPSRGKNC
4R24	CPSDLKDAC
4R4	CRTTRGTKC
4R8	CRMTRNKPC
4R17	CRVSRQNKC
4R9	CAKIDPELC
4R22	CSNIDARAC
3R14	CGGERGKSC

Antitumor Therapy with Liposomal Doxorubicin, Doxorubicin Distribution, Tunel Staining, and *in Vivo* Imaging of Liposome Homing. Mice bearing a subcutaneous tumor were intravenously (iv) treated with HEPES buffer, doxorubicin, liposomal doxorubicin (Lipo-Dox), peptide-conjuaged Lipo-Dox (2 mg of doxorubicin/kg body weight, iv injection, twice a week for total 7 times). Tumor volumes were calculated using the following equation: length × $(\text{width})^2$ × 0.52. Body weights were measured twice a week during the treatment period.

The distribution of doxorubicin in tumor tissue was examined using its autofluorescence (excitation 530−560 nm/emission 573−647 nm). Analysis of tissue apoptosis was conducted by staining tissues with a modified terminal deoxynucleotidyl-transferase mediated UTP end labeling (TUNEL) and rhodamine conjugated antidigoxigenin antibody (Chemicon, Billerica, MA). Tissue sections were incubated with a mounting solution and observed under a fluorescent microscope.

For imaging of liposome homing to tumor, a 100 μL solution of Cy7.5-labeled liposomes without doxorubicin was injected into tumor-bearing mice. After circulation for the indicated time period, *in vivo* near-infrared fluorescence images were taken using Optix explore.

RESULTS

Screening of a Phage Library for Peptides That Selectively Bind to Lung Tumor Cells. A T7 phage library containing CX7C random peptides was screened *in vitro* to enrich phages that bind to H460 cells (a human large cell lung carcinoma cell line). After four rounds of screening, the phage titer was enriched approximately by 600-fold as compared to the first round (Figure 1A). Forty seven phage clones were randomly picked from the third and fourth rounds, and the peptide-coding DNA inserts of the phage clones were sequenced. After analysis of the peptide sequences, eight phage clones (3R5, 3R14, 4R4, 4R8, 4R9, 4R17, 4R22, and 4R24) were chosen for further evaluation (Table 1).

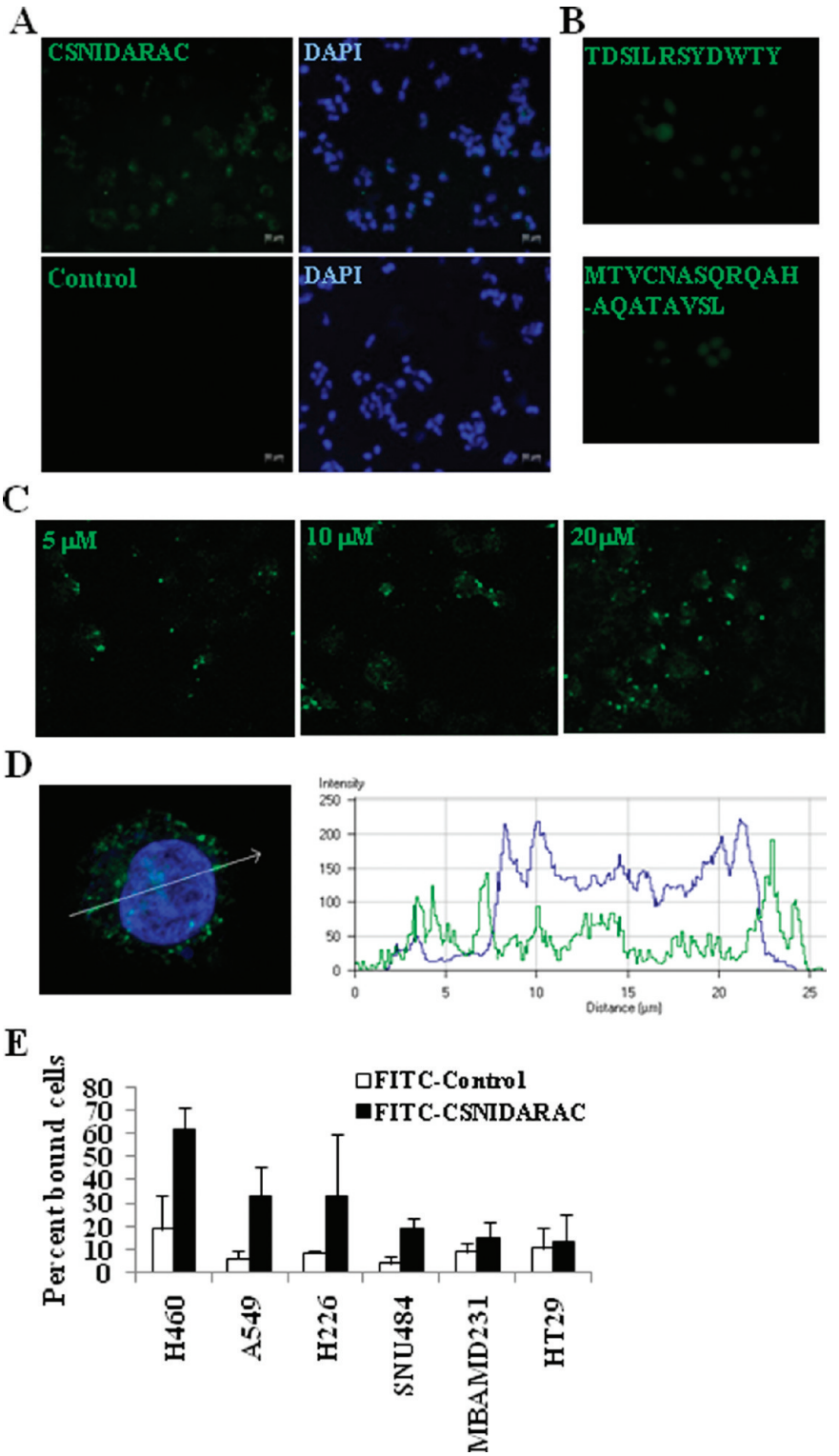

Figure 2. *In vitro* binding of the CSNIDARAC peptide to tumor cells and internalization. (A) Binding assays. A 10 μM solution of FITC-conjugated CSNIDARAC or control peptide (green) was incubated with H460 lung tumor cells at 4 °C for 1 h and then with DAPI (blue) for nuclear staining. Scale bars: 50 μm. (B) Binding of FITC-conjugated TDSILRSYDWTY and MTVCNASQRQAHAQATAVSL peptides (10 μM) to H460 cells. Magnifications, ×400. (C) Internalization assays. FITC-conjugated CSNIDARAC peptide (5, 10, and 20 μM) was incubated with H460 cell at 37 °C for 1 h and observed under a confocal microscopy. Magnifications, ×200. (D) *Z*-Section scanning of a confocal microscopic image, along the direction indicated as an arrow, was taken to examine the intracellular location of FITC-SNIDARAC peptide (10 μM, Left panel). The fluorescence intensity of FITC (green) and DAPI (blue) were shown as a function of distance (μm) (Right panel). Note that the CSNIDARAC peptide is located in the cytoplasm and nucleus. Magnification, ×800. (E) Flow cytometry. FITC-conjugated CSNIDARAC or control peptide (20 μM) was incubated at 4 °C for 1 h with different types of tumor cells in suspension. Cells (H460, A549, and H226, lung tumor; SNU484, stomach tumor, MDA-MB231, breast tumor; HT29, colon tumor) were then subjected to flow cytometry analysis of peptide binding. Bars represent the percent number of fluorescent cells bound with the peptide as mean ± SD of data obtained from three separate experiments.

The cell binding of the individual phage clones was evaluated by phage cell-binding ELISA. Of the eight clones, three phage clones (4R9, 4R17, and 4R22) showed higher binding to H460 cells than other phage clones (Figure 1B). Furthermore, the 4R22 phage clone showed preferential binding to H460 cells over SNU484 cells (a human stomach adenocarcinoma cell line) and BEAS-2B cells (a human normal bronchial epithelial cell line) as compared to the 4R9 and 4R17 phage clones (Figure 1C).

***In Vitro* Binding of the CSNIDARAC Peptide to Lung Tumor Cells.** To investigate the cell binding of the CSNIDARAC peptide that is displayed on the 4R22 phage clone, it was synthesized and conjugated with a green fluorescent FITC dye at the amino terminus. Immunofluorescence analysis demonstrated that the FITC-conjugated CSNIDARAC peptide strongly bound to H460 cells, while little binding was observed with the FITC-conjugated NSSSVDK control peptide, a sequence present in the phage coat protein (Figure 2A). Two previously described peptides, MTVCNASQRQAHAQATAVSL[19] and TDSILRSYDWTY,[20] also bound to H460 cells at a similar binding activity with the CSNIDARAC peptide (Figure 2B). More interestingly, the CSNIDARAC peptide was efficiently internalized into H460 cells within 1 h in a dose-dependent manner (Figure 2C). It was then distributed through the cytoplasm and nucleus, as shown by the *Z*-section scanning of the cells using a confocal microscope (Figure 2D).

Next, the binding of the CSNIDARAC peptide to H460 cells versus different types of tumor cells was measured by flow cytometry analysis. The percentage of the CSNIDARAC peptide-bound H460 cells was 62 ± 10% (Figure 2E). In addition, the percentages of the CSNIDARAC peptide-bound A549 cells (a human lung adenocarcinoma cell line) and H226 cells (a human lung squamous carcinoma cell line) were 35 ± 13% and 35 ± 28%, respectively (Figure 2E). On the other hand, the percentages of CSNIDARAC peptide-bound SNU484 cells, MDA-MB-231 cells (a human breast adenocarcinoma cell line), and HT29 cells (a human colon adenocarcinoma cell line) were 19 ± 5%, 16 ± 7%, and 14 ± 13%, respectively (Figure 2E). These results indicate that the binding of the CSNIDARAC peptide to other types of tumor cells is relatively weak when compared to the binding to lung tumor cells.

***In Vivo* Imaging of Tumor by Homing of the CSNIDARAC Peptide to Lung Tumor.** It was important to determine whether the CSNIDARAC peptide homes to lung tumor and allows the *in vivo* detection and imaging of the tumor. *In vivo* fluorescence imaging of tumor site demonstrated that much higher levels of fluorescence signals were detected 1 h after intravenous injection at the H460 tumor of mice injected with the FITC-SNIDARAC peptide than with the FITC-control peptide (Figure 3A, right panels). *Ex vivo* examination of tumors further demonstrated higher levels of fluorescence signals at the tumor of mice injected with the CSNIDARAC peptide than the control peptide (Figure 3B). Minimal levels of fluorescence signals were observed at the liver, lung, spleen, and heart (Figure 3B), suggesting that the nonspecific homing of the peptide to other organs, including normal lung tissues, is negligible. However, strong florescence signals were detected in the kidney of mice injected with either the CSNIDARAC or control peptide at 2 h after injection (Figure 3B), suggesting the excretion of peptides out of the body through the urine.

Consistent with the findings of *in vivo* and *ex vivo* imaging, histological examination of frozen sections of tissue demonstrated that the CSNIDARAC peptide was abundantly localized at

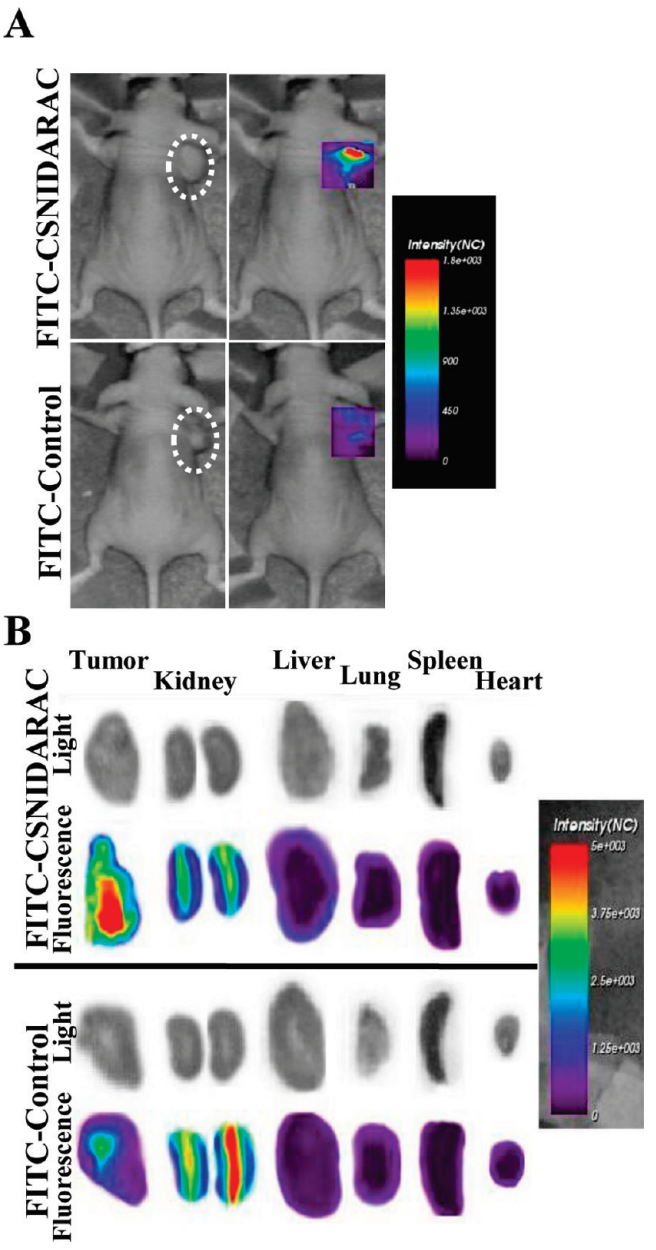

Figure 3. *In vivo* imaging of lung tumor by homing of the CSNIDARAC peptide to tumor. (A) FITC-conjugated CSNIDARAC or control peptide was intravenously injected into mice bearing H460 tumor. *In vivo* fluorescence images were taken 1 h after circulation of each peptide (right panels). Light images were taken before injection, and dotted circles indicate the location of tumor (left panels). (B) Light and *ex vivo* fluorescence and images of tumors and organs that were isolated from mice after 2 h circulation of each peptide. Scale bars indicate the normalized fluorescence intensity (NC).

tumor tissue (Figure 4A and C), while the control peptide was little detected (Figure 4B). Moreover, the levels of the CSNIDARAC peptide at control organs such as the liver, lung, and spleen were minimal (Figure 4D−F).

The CSNIDARAC Peptide-Targeted Delivery of Liposomal Doxorubicin to Lung Tumor. In order to examine whether the CSNIDARAC peptide can enhance the delivery of nanoparticle therapeutics to lung tumor, the peptide was conjugated to the terminal −OH groups on PEGylated (1.3 mol % of total lipids)

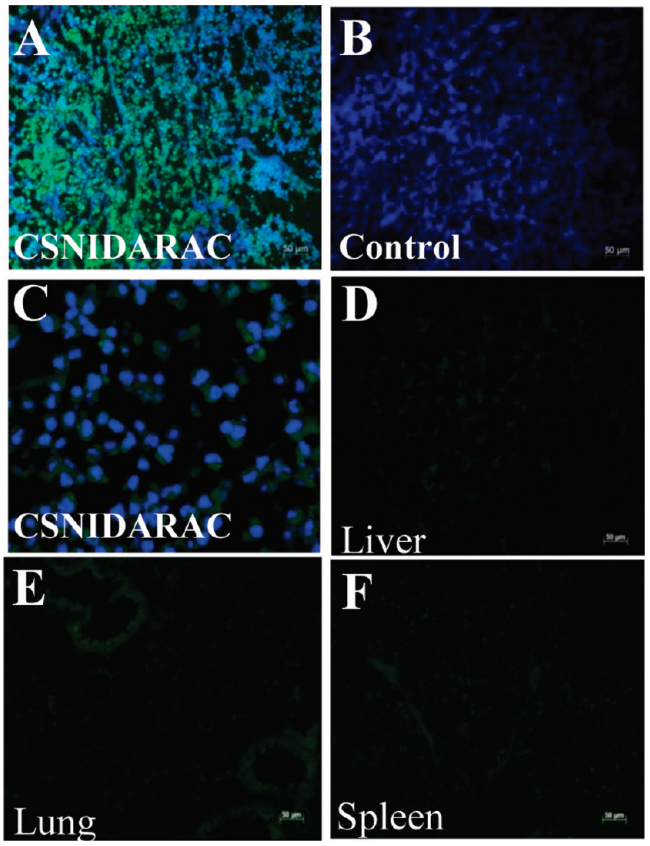

Figure 4. Histologic analysis of the CSNIDARAC peptide homing. Tumors and organs were isolated from mice after 2 h circulation of FITC-conjugated CSNIDARAC or control peptide. Sections of frozen tissues were incubated with a mounting medium containing DAPI for nuclear staining and observed under a fluorescence microscope (A, B and D−F) and confocal microscope (C). (A, C) FITC−CSNIDARAC peptide (green) at tumor tissue and DAPI (blue). (B) FITC-control peptide (green) at tumor tissue and DAPI (blue). FITC−CSNIDARAC peptide at the liver (D), lung (E), and spleen (F). Scale bars: 50 μm. (C) Magnifications: ×400.

liposomal doxorubicin (Lipo-Dox) using PEG as a spacer or linker (particle diameter, 200 nm). When intravenously administered into H460 lung tumor-bearing mice, the CSNIDARAC peptide-targeted Lipo-Dox inhibited tumor growth more efficiently than untargeted Lipo-Dox and free doxorubicin given at the equivalent dose of doxorubicin (2 mg/kg body weight; Figure 5A). Body weights of untreated and treated groups were not significantly changed by the treatment (Figure 5B).

To examine the *in vivo* homing of the peptide-directed liposomes (drug carrier) to tumor, they were labeled with the Cy7.5 near-infrared dye and then intravenously injected into tumor-bearing mice. Whole body scanning of chest and abdomen at 2 h after injection revealed that higher levels of fluorescence signals were observed at tumor of mice treated with the CSNIDARAC-targeted liposomes than with untargeted liposomes (Figure 5C, right panels).

Next, it was examined whether the delivery of doxorubicin (payload) and the subsequent apoptosis of tumor cells were actually enhanced by the targeting of liposomal doxorubicin to tumor. Fluorescence microscopic analysis of tumor tissues at the end of treatment demonstrated that the amount of doxorubicin, determined by its autofluorescence level, was higher at tumor tissue of mice treated with the CSNIDARAC-targeted Lipo-Dox than with untargeted Lipo-Dox or free doxorubicin (Figure 5D). In the same context, the levels of apoptosis, measured by TUNEL staining, were higher in tumor tissue treated with targeted liposomes than with untargeted liposomes or free doxorubicin (Figure 5E). Little apoptosis, on the other hand, was observed in the liver tissue as a control organ when treated with the CSNIDARAC-targeted Lipo-Dox (Figure 5E).

DISCUSSION

Using a phage displayed-peptide library, we identified the CSNIDARAC peptide that was able to bind to lung tumor cells, such as H460, A549 and H226 cells. Its binding was preferential to lung tumor cells, since weak binding was observed with other types of tumor cells such as stomach, breast, and colon tumor cells. *In vivo* imaging signals were detected at lung tumor of mice by homing of the fluorescent CSNIDARAC peptide. The labeling of CSNIDARAC peptide as a targeting probe on PEGylated liposomal doxorubicin was able to enhance its antitumor therapeutic efficacy compared to free doxorubicin and untargeted liposomal doxorubicin. These findings show that the CSNIDARAC peptide is a promising targeting probe for imaging and drug delivery to lung tumor.

Lung cancers are divided into small cell lung cancer and non-small cell lung cancer. Non-small cell lung cancer is further divided into adenocarcinoma (e.g, A549 and CL1−5 cells), squamous cell carcinoma (e.g., H226 cells), and large cell carcinoma (e.g., H460 cells). Peptides that preferentially bind to lung adenocarcinoma cells have been previously described. For example, the TDSILRSYDWTY peptide was isolated for binding to CL1−5 cells.[20] When labeled on liposomes, it enhanced the delivery of liposomal doxorubicin to lung tumor and increased its antitumor growth activity. Another example is the MTVCNASQRQAHAQATAVSL peptide that was identified as binding to A549 cells.[19] Although the previously described peptides were selected for binding to CL1−5 or A549 adenocarcinoma cells and there was no homology in sequence compared to the CSNIDARAC peptide, we observed that all of them were able to bind to H460 large cell carcinoma cells with a similar binding activity. Peptides with similar targeting behavior but containing different sequences might be identified depending on the cell type and phage library used for screening. They may bind to different receptors or recognize different epitopes in the same receptor on target cells. It may be interesting to examine whether a multimeric ligand composed of the three different peptide sequences would show an enhanced, synergistic targeting activity to lung tumor than a multimeric ligand composed of only one type of peptide sequence.

PEG-conjugated liposomal doxorubicin has several advantages over free doxorubicin. The primary advantage of PEGylated liposomal doxorubicin in cancer treatment is the reduction of cardiotoxicity, which is the main side effect of doxorubicin.[5,22,23] This led Doxil, a representative example of PEGylated liposomal doxorubicin, to be approved for the treatment of cancer such as AIDS-related Kaposi's sarcoma and ovarian cancer.[5] Second, it can circulate through the bloodstream for 100 times longer than free doxorubicin (half-life: 84 and 0.8 h, respectively).[24] This longer circulation of nanoparticles may enhance the accumulation of drugs into tumor and thus increase therapeutic efficacy. Third, nanoparticle carriers may be entrapped within the tumor tissue due to the EPR (enhanced permeability and retention)

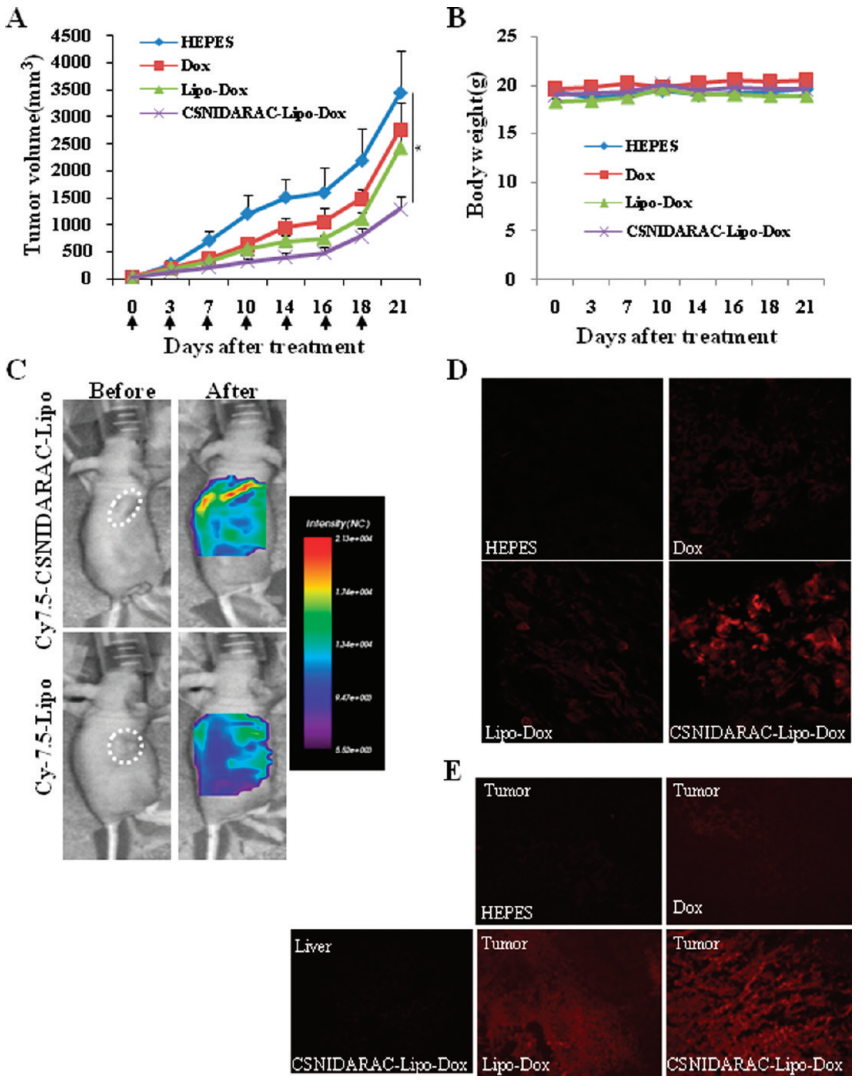

Figure 5. The CSNIDARAC peptide-targeted delivery of liposomal doxorubicin to lung tumor. (A) Mice bearing a tumor (approximately 3 mm in diameter) were treated by the intravenous injection of HEPES buffer, free doxorubicin (Dox), liposomal doxorubicin (Lipo-Dox), and the CSNIDARAC-labeled Lipo-Dox (2 mg of doxorubicin/kg body weight at days indicated as arrows for total 7 times). Data represent tumor volumes as mean ± SD (n = 5). *, $P < 0.05$ by Student's t-test. (B) Body weights in grams of mice studied in (A). (C) Cy7.5-labeled liposomes were intravenously injected into tumor-bearing mice and *in vivo* near-infrared fluorescence images were taken 2 h after circulation of liposomes (right panels). Light images were taken before injection, and dotted circles indicate the location of tumor (left panels). A scale bar indicates the normalized fluorescence intensity (NC). (D) Tumors in panel A were isolated and the distribution of doxorubicin in tumor tissue treated with the indicated agents was examined using the autofluorescence of doxorubicin. (E) TUNEL staining of tumor tissues and the liver tissue treated with the indicated agents. Magnifications, ×200.

effect and then be taken up into tumor cells by endocytosis, overcoming the efflux pump-mediated multidrug resistance, or MDR, common to many tumor cells.[5,25]

On top of that, the therapeutic efficacy of liposomal doxorubicin can be further increased by conjugating targeting ligands on their surface. It has been suggested that the key role of targeting ligands is to enhance the internalization of nanoparticles into cells.[26,27] In general, PEGylation of about 5−20 mol % of total lipids has been used to achieve long blood circulation of liposomes.[28,29] In this study, however, we used a low mol % (1.3 mol % of total lipids) of PEG as a spacer molecule to minimize the interaction of the targeting peptide probe with the surface of liposomes, rather than to confer the long-circulating property. *In vivo* imaging of fluorescent liposomes demonstrated that the accumulation of the CSNIDARAC-directed liposomes, but not untargeted liposomes, at tumor was already remarkable 2 h after circulation. This was much earlier than expected for the accumulation of nanoparticles due to the EPR effect at tumor tissue, which takes about 6 h or longer to peak.[30] In the same context with the low levels of accumulation at tumor, we observed that the untargeted liposomal doxorubicin had a minimal level of antitumor activity, which was similar to that of an equivalent dose of doxorubicin alone. It remains a future direction to establish the relationship between the mol % of the CSNIDARAC peptide−PEG conjugate and the therapeutic efficacy. When peptide ligands are conjugated via a PEG spacer to the surfaces of nanoparticles, they tend to be protected from proteolysis, while free peptides tend to be easily degraded by proteases.[31] Moreover, multiple peptides could be displayed on each nanoparticle, and this may enhance the targeting activity of the nanoparticles, even when a

peptide ligand with a low affinity is used (multivalency effect).[32] Taken together, peptide-guided liposomal doxorubicin would be a promising approach for drug delivery and antitumor therapy.

Phage display may play a role as a platform technology for identifying ligand mimetics and biomarkers on cell surfaces. For example, the CRGRRST peptide that was selected for homing to blood vessels of pancreatic islet tumors was shown to share the RGRRS motif with platelet-derived growth factor-B (PDGF-B) and to bind to PDGF receptor-beta on endothelial cells.[33] Protein database search of the CSNIDARAC sequence reveals proteins that contain homologous motifs. It is homologous, for example, with the ^{868}CSDID^{872} sequence of human EGF that plays an important role for cell proliferation via binding to EGF receptor. EGF is a polypeptide of 53 amino acids, which is derived by proteolytic cleavage of pre-proEGF between the residue 971 and 1023.[34] In order to better understand how the CSNIDARAC peptide can target lung tumor cells, it remains to identify its cognate receptor on the surface of the cells. The receptor may be either a known protein overexpressed on lung tumor cells (e.g., EGF receptor) or a novel protein (or biomarker) with an unknown function.

Early detection of lung cancer is still a major challenge. It remains to be determined whether CSNIDARAC peptide-guided PET and magnetic resonance (MR) imaging can enhance imaging signals and provide earlier detection of lung cancer than conventional, untargeted imaging. It is expected that the peptide-guided imaging agents will penetrate into lung tumor tissues faster than antibody-guided agents. Moreover, multifunctional nanoparticles equipped with drugs (small molecules or siRNA), imaging agents (fluorescence, PET, and MR), and the CSNIDARAC peptide as a targeting moiety may be useful for theranostic strategy (therapy combined with diagnosis).

AUTHOR INFORMATION

Corresponding Author

*B.-H.L.: Department of Biochemistry and Cell Biology, School of Medicine, Kyungpook National University, 101 Dongin-Dong, Jung-gu, Daegu, 700-421, Korea; tel, +82-53-420-4824; fax, +82-53-422-1466; e-mail, leebh@knu.ac.kr.

ACKNOWLEDGMENT

This work was supported by the grant from the National R&D Program for Cancer Control, Ministry for Health, Welfare and Family affairs, Republic of Korea (0720550-2), Basic Science Research Program through the National Research Foundation of Korea (NRF) funded by the Ministry of Education, Science and Technology (R11-2008-044-03002-0), and WCU Program through the NRF funded by the Ministry of Education, Science and Technology (R33-10054).

REFERENCES

(1) Jemal, A.; Siegel, R.; Ward, E.; Hao, Y.; Xu, J.; Murray, T.; Thun, M. J. Cancer statistics, 2008. *CA Cancer J. Clin.* **2008**, *58*, 71–96.

(2) Fukuoka, M.; Yano, S.; Giaccone, G.; Tamura, T.; Nakagawa, K.; Douillard, J. Y.; Nishiwaki, Y.; Vansteenkiste, J.; Kudoh, S.; Rischin, D.; Eek, R.; Horai, T.; Noda, K.; Takata, I.; Smit, E.; Averbuch, S.; Macleod, A.; Feyereislova, A.; Dong, R. P.; Baselga, J. Multi-institutional randomized phase II trial of gefitinib for previously treated patients with advanced non-small-cell lung cancer (The IDEAL 1 Trial) [corrected]. *J. Clin. Oncol.* **2003**, *21*, 2237–2246.

(3) Paez, J. G.; Janne, P. A.; Lee, J. C.; Tracy, S.; Greulich, H.; Gabriel, S.; Herman, P.; Kaye, F. J.; Lindeman, N.; Boggon, T. J.; Naoki, K.; Sasaki, H.; Fujii, Y.; Eck, M. J.; Sellers, W. R.; Johnson, B. E.; Meyerson, M. EGFR mutations in lung cancer: correlation with clinical response to gefitinib therapy. *Science* **2004**, *304*, 1497–1500.

(4) Gatter, K. C.; Brown, G.; Trowbridge, I. S.; Woolston, R. E.; Mason, D. Y. Transferrin receptors in human tissues: their distribution and possible clinical relevance. *J. Clin. Pathol.* **1983**, *36*, 539–545.

(5) Davis, M. E.; Chen, Z. G.; Shin, D. M. Nanoparticle therapeutics: an emerging treatment modality for cancer. *Nat. Rev. Drug Discovery* **2008**, *7*, 771–782.

(6) Farokhzad, O. C.; Cheng, J.; Teply, B. A.; Sherifi, I.; Jon, S.; Kantoff, P. W.; Richie, J. P.; Langer, R. Targeted nanoparticle-aptamer bioconjugates for cancer chemotherapy in vivo. *Proc. Natl. Acad. Sci. U.S.A.* **2006**, *103*, 6315–6320.

(7) Arap, W.; Pasqualini, R.; Ruoslahti, E. Cancer treatment by targeted drug delivery to tumor vasculature in a mouse model. *Science* **1998**, *279*, 377–380.

(8) Bauer, W.; Briner, U.; Doepfner, W.; Haller, R.; Huguenin, R.; Marbach, P.; Petcher, T. J. Pless, SMS 201−995: a very potent and selective octapeptide analogue of somatostatin with prolonged action. *Life Sci.* **1982**, *31*, 1133–1140.

(9) Henze, M.; Schuhmacher, J.; Dimitrakopoulou-Strauss, A.; Strauss, L. G.; Macke, H. R.; Eisenhut, M.; Haberkorn, U. Exceptional increase in somatostatin receptor expression in pancreatic neuroendocrine tumour, visualised with (68)Ga-DOTATOC PET. *Eur. J. Nucl. Med. Mol. Imaging* **2004**, *31*, 466.

(10) Bodei, L.; Cremonesi, M.; Zoboli, S.; Grana, C.; Bartolomei, M.; Rocca, P.; Caracciolo, M.; Macke, H. R.; Chinol, M.; Paganelli, G. Receptor-mediated radionuclide therapy with 90Y-DOTATOC in association with amino acid infusion: a phase I study. *Eur. J. Nucl. Med. Mol. Imaging* **2003**, *30*, 207–216.

(11) Zhang, J.; Jin, W.; Wang, X.; Wang, J.; Zhang, X.; Zhang, Q. A Novel Octreotide Modified Lipid Vesicle Improved the Anticancer Efficacy of Doxorubicin in Somatostatin Receptor 2 Positive Tumor Models. *Mol. Pharmaceutics* **2010**, *7*, 1159–1168.

(12) Ladner, R. C.; Sato, A. K.; Gorzelany, J.; de Souza, M. Phage display-derived peptides as therapeutic alternatives to antibodies. *Drug Discovery Today* **2004**, *9*, 525–529.

(13) Chen, X.; Tohme, M.; Park, R.; Hou, Y.; Bading, J. R.; Conti, P. S. Micro-PET imaging of alphavbeta3-integrin expression with 18F-labeled dimeric RGD peptide. *Mol. Imaging* **2004**, *3*, 96–104.

(14) Liu, S. Radiolabeled multimeric cyclic RGD peptides as integrin alphavbeta3 targeted radiotracers for tumor imaging. *Mol. Pharmaceutics* **2006**, *3*, 472–487.

(15) Hoffman, J. A.; Giraudo, E.; Singh, M.; Zhang, L.; Inoue, M.; Porkka, K.; Hanahan, D.; Ruoslahti, E. Progressive vascular changes in a transgenic mouse model of squamous cell carcinoma. *Cancer Cell* **2003**, *4*, 383–391.

(16) Hong, H. Y.; Choi, J. S.; Kim, Y. J.; Lee, H. Y.; Kwak, W.; Yoo, J.; Lee, J. T.; Kwon, T. H.; Kim, I. S.; Han, H. S.; Lee, B. H. Detection of apoptosis in a rat model of focal cerebral ischemia using a homing peptide selected from in vivo phage display. *J. Controlled Release* **2008**, *131*, 167–172.

(17) Hsiung, P. L.; Hardy, J.; Friedland, S.; Soetikno, R.; Du, C. B.; Wu, A. P.; Sahbaie, P.; Crawford, J. M.; Lowe, A. W.; Contag, C. H.; Wang, T. D. Detection of colonic dysplasia in vivo using a targeted heptapeptide and confocal microendoscopy. *Nat. Med.* **2008**, *14*, 454–458.

(18) Lee, S. M.; Lee, E. J.; Hong, H. Y.; Kwon, M. K.; Kwon, T. H.; Choi, J. Y.; Park, R. W.; Kwon, T. G.; Yoo, E. S.; Yoon, G. S.; Kim, I. S.; Ruoslahti, E.; Lee, B. H. Targeting bladder tumor cells in vivo and in the urine with a peptide identified by phage display. *Mol. Cancer Res.* **2007**, *5*, 11–19.

(19) Oyama, T.; Sykes, K. F.; Samli, K. N.; Minna, J. D.; Johnston, S. A.; Brown, K. C. Isolation of lung tumor specific peptides from a random peptide library: generation of diagnostic and cell-targeting reagents. *Cancer Lett.* **2003**, *202*, 219–230.

(20) Chang, D. K.; Lin, C. T.; Wu, C. H.; Wu, H. C. A novel peptide enhances therapeutic efficacy of liposomal anti-cancer drugs in mice models of human lung cancer. *PLoS One* **2009**, *4*, e4171.

(21) Wu, C.; Lo, S. L.; Boulaire, J.; Hong, M. L.; Beh, H. M.; Leung, D. S.; Wang, S. A peptide-based carrier for intracellular delivery of proteins into malignant glial cells in vitro. *J. Controlled Release* **2008**, *130*, 140–145.

(22) Rahman, A. M.; Yusuf, S. W.; Ewer, M. S. Anthracycline-induced cardiotoxicity and the cardiac-sparing effect of liposomal formulation. *Int. J. Nanomed.* **2007**, *2*, 567–583.

(23) Batist, G. Cardiac safety of liposomal anthracyclines. *Cardiovasc. Toxicol.* **2007**, *7*, 72–74.

(24) Sutton, D.; Nasongkla, N.; Blanco, E.; Gao, J. Functionalized micellar systems for cancer targeted drug delivery. *Pharm. Res.* **2007**, *24*, 1029–1046.

(25) Cuvier, C.; Roblot-Treupel, L.; Millot, J. M.; Lizard, G.; Chevillard, S.; Manfait, M.; Couvreur, P.; Poupon, M. F. Doxorubicin-loaded nanospheres bypass tumor cell multidrug resistance. *Biochem. Pharmacol.* **1992**, *44*, 509–517.

(26) Kirpotin, D. B.; Drummond, D. C.; Shao, Y.; Shalaby, M. R.; Hong, K.; Nielsen, U. B.; Marks, J. D.; Benz, C. C.; Park, J. W. Antibody targeting of long-circulating lipidic nanoparticles does not increase tumor localization but does increase internalization in animal models. *Cancer Res.* **2006**, *66*, 6732–6740.

(27) Bartlett, D. W.; Su, H.; Hildebrandt, I. J.; Weber, W. A.; Davis, M. E. Impact of tumor-specific targeting on the biodistribution and efficacy of siRNA nanoparticles measured by multimodality in vivo imaging. *Proc. Natl. Acad. Sci. U.S.A.* **2007**, *104*, 15549–15554.

(28) Chow, T. H.; Lin, Y. Y.; Hwang, J. J.; Wang, H. E.; Tseng, Y. L.; Wang, S. J.; Liu, R. S.; Lin, W. J.; Yang, C. S.; Ting, G. Improvement of biodistribution and therapeutic index via increase of polyethylene glycol on drug-carrying liposomes in an HT-29/luc xenografted mouse model. *Anticancer Res.* **2009**, *29*, 2111–2120.

(29) Ho, E. A.; Ramsay, E.; Ginj, M.; Anantha, M.; Bregman, I.; Sy, J.; Woo, J.; Osooly-Talesh, M.; Yapp, D. T.; Bally, M. B. Characterization of cationic liposome formulations designed to exhibit extended plasma residence times and tumor vasculature targeting properties. *J. Pharm. Sci.* **2010**, *99*, 2839–2853.

(30) Maeda, H.; Fang, J.; Inutsuka, T.; Kitamoto, Y. Vascular permeability enhancement in solid tumor: various factors, mechanisms involved and its implications. *Int. Immunopharmacol.* **2003**, *3*, 319–328.

(31) Nilsson, F.; Tarli, L.; Viti, F.; Neri, D. The use of phage display for the development of tumour targeting agents. *Adv. Drug Delivery Rev.* **2000**, *43*, 165–196.

(32) Zhou, Y.; Drummond, D. C.; Zou, H.; Hayes, M. E.; Adams, G. P.; Kirpotin, D. B.; Marks, J. D. Impact of single-chain Fv antibody fragment affinity on nanoparticle targeting of epidermal growth factor receptor-expressing tumor cells. *J. Mol. Biol.* **2007**, *371*, 934–947.

(33) Joyce, J. A.; Laakkonen, P.; Bernasconi, M.; Bergers, G.; Ruoslahti, E.; Hanahan, D. Stage-specific vascular markers revealed by phage display in a mouse model of pancreatic islet tumorigenesis. *Cancer Cell* **2003**, *4*, 393–403.

(34) Harris, R. C.; Chung, E.; Coffey, R. J. EGF receptor ligands. *Exp. Cell Res.* **2003**, *284*, 2–13.